Evidence for Biological Effects in the Radiosensitization of Leukemia

Cell Lines by PEGylated Gold Nanoparticles

Benjamin P. Coughlin, Paul T. Lawrence, Irene Lui, Christopher J. Luby, Daniel J.

Spencer, E. Charles H. Sykes, and Charles R. Mace*

ADDRESS: Department of Chemistry, Tufts University, 62 Talbot Ave., Medford, MA,

USA, 02155

KEYWORDS: Gold nanoparticles, leukemia, radiation therapy, radiosensitizers

*Corresponding author email: charles.mace@tufts.edu

ABSTRACT

Gold nanoparticles (Au NPs) are promising radiosensitizers for cancer therapy. While the

radiosensitizing effects of Au NPs have been shown in many epithelial cancers, there are no

documented cases of their use in cells of hematopoietic origin, which constitute ~10% of all

cancer cases and are frequently treated using radiation therapy. In this work, we measure the

uptake of polyethylene glycol-coated (PEGylated) Au NPs (5 nm core diameter) in HL-60 II and

Jurkat D1.1 cells using flow cytometry and ICP-AES. Electronic cell counting, metabolic activity

assays, and DNA synthesis assays reveal cell-line specific radiosensitization that is

independent of the number of internalized nanoparticles. The high SER value for the HL-60 II

cell line (1.33 at 5 Gy) points to a dominant biological mechanism.

INTRODUCTION

Leukemia is a hematological malignancy characterized by the uncontrolled, clonal growth of white blood cells (Soni, 2015; Guo, 2014). In acute disease, disruption of hematopoiesis leads to anemia, immunodeficiency, and decreasing platelet counts. Traditional approaches to management of leukemia include chemotherapy and hematopoietic stem cell transplant (Gupta, Tallman, and Weisdorf 2011; Wiernik et al. 1992). Most patients present with disseminated disease, characterized by large numbers of blast cells in both marrow and circulation. While radiation therapy is commonly used in the treatment of tumors, where localized dose deposition can be better controlled, the use of external radiation therapy is often impractical due to offtarget toxicities in the treatment of leukemia. Nevertheless, some types of hematological malignancies (e.g., Sezary syndrome (Duvic, 2010; Hughes, 2015), myeloid sarcoma (Tsimberidou, 2003), and lymphoma) may present as cutaneous patches of malignant cells or solid tumors. Additionally, total bodv irradiation often even used decrease the number of leukemic cells prior to stem cell transplant (Uckun, 2015; Uckun, Myers, Ma, et al., 2015). For these reasons, there is active interest in finding new ways to increase the sensitivity of leukemia cells to ionizing radiation, which in turn would decrease tumor burden and improve the chances for sustained remission.

Heavy metal nanoparticles have been shown to sensitize cancer cells to ionizing radiation in vitro and in vivo, leading to significantly more cell death or tumor reduction than by radiation therapy alone (Butterworth, 2012; Schuemann, 2016). At first, the radiosensitizing effects of metal NPs were hypothesized to result from increased X-ray absorption (Hainfeld, 2008) in heavy metal nanoparticles. The production of photoelectrons and then Auger and low energy electrons by inelastic scattering events is one explanation for the radiosensitizing effects (Kouass Sahbani, 2015; J. Liu, 2015; Alizadeh, 2015). Nevertheless, there is no definitive proof of this hypothesis and many contradictory results exist in the literature. In recent years, it has become evident that the disruption of biological processes in the cell (e.g., cell cycle arrest

(Roa, 2009) or induction of autophagy (Zhu, 2017)) may also contribute to the dose enhancing effects of metal NPs. Of the metallic nanoparticles, gold nanoparticles (Au NPs) are by far the most widely studied. Au NPs have been shown to sensitize cancer cells at a wide range of photon energies (Ngwa, 2013; Berbeco, 2012) and surface coatings. Importantly, Au NPs are generally non-toxic (Pan, 2007; Connor, 2005), may be modified in situ by thiol-containing molecules (Ulman, 1996; Vericat, 2010), and enter cancerous tissue due to the enhanced permeability and retention (EPR) effect (Jain, 2012).

Here, we functionalize 5 nm Au NPs with polyethylene glycol (PEG), a well-characterized, biocompatible polymer, which is known to decrease protein adsorption and immune responses to colloidal particles. We investigate the ability of these bioconjugates to radiosensitize two leukemia cell lines, Jurkat D1.1 and HL-60 II (Keppler, 1999), which were established from patients with acute T-cell leukemia and acute promyelocytic leukemia, respectively. While similar experiments have been performed with epithelial cells (Her, 2017), we make the first measurements showing decreased cell survival and a clear radiosensitizing effect in a blood cancer cell type.

Experimental

Materials

Gold colloid was purchased from Ted Pella (Redding, CA). mPEG-thiol (2,000 M.W. average) and H₂N-nPEG-thiol (1,000 M.W. average) were purchased from Laysan Bio (Arab, AL) as solid powders. Cy5-NHS ester was purchased from Molecular Probes (Eugene, OR). Cell culture medium and fetal bovine serum (FBS) were purchased from Gibco. DAPI, Presto Blue, and Click-iT EdU reagents and assay kits were purchased from Thermo Fisher Scientific. All other materials were purchased from Sigma Aldrich (St. Louis, MO).

Nanoparticle Preparation

Nanoparticles were functionalized by adding a 87:13 ratio of mPEG-thiol (2 mM) and H_2N_2 PEG-thiol (2 mM) to 3 mL of as-purchased Au NP suspension. The ligands were incubated with

the NPs for 24 h at room temperature, protected from light. The NPs were concentrated using an Amicon filter tube (30 kDa M.W. cutoff) and washed in buffer containing 0.01% w/v sodium citrate and 0.01% v/v tween-20 to remove unbound PEG. For analysis by fluorescence microscopy, the amine-terminated PEG molecules were labelled with Cy5-NHS ester according to manufacturer's protocols. Briefly, 10 µL of 15 µM Cy5-NHS ester in DMSO was added to 90 µL of 0.1 µM PEGylated Au NPs in sodium bicarbonate buffer, adjusted to pH 8.4. The suspension was allowed to react overnight at 4 °C protected from light. The NP suspension was washed and concentrated again using an Amicon filter tube, until flowthrough showed no signs of free Cy5. Before cell culture use NPs were resuspended in RPMI 1640 (10% FBS) and filtered using a 0.22 µm filter. Nanoparticle concentration was measured after filtration.

Cell Culture

Jurkat D1.1 cells were purchased from ATCC (CRL-10915). The HL-60 II cell line was a kind gift from Prof. Michael Pawlita (Keppler 1999). Both cell lines were cultured in RPMI 1640 supplemented with 10% FBS and 1% penicillin/streptomycin in a humid environment at 5% CO₂ and 37 °C. Cells were passaged when the concentration of cells was ~5×10⁵ mL⁻¹ and all experimental data were taken when the cells had been passaged between 7–15 times, with cells cultured no longer than 6 weeks after removal from liquid nitrogen storage.

Nanoparticle Characterization

UV-Vis spectra were measured with a Genesys UV-Vis spectrophotometer (Thermo Fisher Scientific). Dynamic light scattering (DLS) measurements were performed using a Malvern Zetasizer Nano-ZS. For DLS measurements, non-functionalized NPs were analyzed in the buffer supplied by the manufacturer (containing sodium citrate) diluted with 18.2 M Ω H $_2$ O while PEGylated NPs were resuspended in 18.2 M Ω H $_2$ O after centrifugation. Both samples were filtered with a 0.22 μ m filter prior to analysis. Measurements were made in 173° backscattering mode.

Fluorescence Microscopy

Jurkat D1.1 and HL 60 II cells were incubated to a concentration of 2×10^5 cells mL⁻¹ in T-75 flasks and then were spiked with Au NPs to achieve a concentration of 15 nM. After 24 h incubation, cells were pelleted, washed thrice with 1x warm PBS, and fixed in 4% paraformaldehyde for 30 m at 37 °C. Afterwards, cells were pelleted again, washed in warm PBS and resuspended in 500 μ L of DAPI (2 μ g mL⁻¹) solution and were allowed to incubate for 30 min at room temperature protected from light. Cells were pelleted, DAPI solution was removed, and the cells were washed with warm PBS. After the last centrifugation step, cells were resuspended in 30 μ L of warm cell culture medium (without phenol red), and this volume was added to a glass cover slip for imaging. Fluorescence images were recorded using a Leica DMi8 microscope equipped with an Andor Revolution DSD2 confocal imaging system and a 63x water immersion objective (Leica). All images were processed using Imaris (bitplane).

Flow Cytometry

All flow cytometry data were acquired using a Guava easyCyte Flow Cytometer 6HT-2L (EMD-Millipore). Data were gated for single cells and at least 3×10^4 events were counted for each run.

ICP-AES

Whole cell ICP analysis was performed by first pelleting the cells (5 min at 200 g), removing the supernatant, and washing thrice with PBS. Cells were counted before the last centrifugation step to minimize losses due to pipetting. The cell pellets were lysed with ~1 mL of concentrated nitric acid (using a transfer pipet) and quantitatively transferred to a 10 mL round bottom flask for digestion with additional concentrated nitric washes as needed. The round bottom flasks were immersed in an oil bath (maintained at 100-130 °C) for 2 h. After cooling, the clear cell lysates were quantitatively transferred to 3 mL volumetric flasks and the volume was adjusted using 5% nitric acid. The samples were analyzed using a Prodigy/Prism High Dispersion ICP-AES (Teledyne Leeman Labs). The introduction conditions for the instrument were as follows:

SeaSpray concentric nebulizer, 0.2 L/min auxiliary argon flow, 18 L/min coolant gas flow, 1.4 mL/min sample flow, and 32 PSI nebulizer gas pressure. Plasma was set to 1.1 kW with an optics purge flow of 0.7 L/min. Measurement readings were performed with a 40 s uptake delay and axial mode was used for all measurements. Three integrations were performed at 30 s each. Calibration curves were constructed using elemental gold ICP standards and elemental indium was used as an internal standard for all calibrations, blanks, and sample measurements. *Cell Irradiations*

All irradiations were performed using an X-Rad 320 Precision X-ray machine (PXi, North Branford, CT) at 320 kVp X-ray energy working at 12.5 mA current. The filter used for irradiations was composed of 1.5 mm Al, 0.25 mm Cu, and 0.75 mm Sn to give a dose rate of 101 cGy min⁻¹ at a working distance of 50 cm. Cells were irradiated for the appropriate length of time to achieve doses of 1, 3, and 5 Gy. To control for local temperature fluctuations, control cells were sham irradiated by leaving them out on the bench for the same amount of time as the 5 Gy sample. For all irradiation experiments, cells were transported in sealed 96 well plates from Tufts University to Massachusetts General Hospital in a humid container at 37 °C. All cells were plated at a concentration of 2 × 10⁴ cells mL⁻¹ 24 h prior to irradiation. When the color of the non-irradiated cells' medium began to change, the medium for all cells was changed (~ 3 d). *Cell Counts*

All cell counts were performed with a Countess II Automated Cell Counter (Thermo Fisher Scientific). The sensitivity enhancement ratio was defined as the ratio of control cells to Au NP treated cells at 5 days post irradiation. To avoid sampling biases associated with counting cells in larger tissue culture dishes (e.g., T-25 flasks), 96 well plates were used for cell growth curves as this allowed for facile homogenization and sampling at each time point. Prior to counting, the volume of medium was adjusted by with a volumetric pipette to 200 µL.

Resazurin Reduction Assay/MTT Assay

The Alamar Blue viability assay was performed using the commercially available Presto Blue reagent according to the manufacturer's protocol. For the cells to be analyzed, medium was removed and replaced with fresh medium (without phenol red), at which time 8 µL of Presto Blue reagent was spiked into each well for analysis and also into wells containing only medium to blank the plate reader. Fluorescence measurements were measured at 590 nm.

MTT assays were performed by the method of Freshney with modifications. Cells were exposed to nanoparticles for 24 h. After an additional doubling time, cells were incubated with 5 mg mL⁻¹ MTT reagent (Thermo Fisher scientific) in RPMI 1640 without phenol red indicator. After 2 h, cells were pelleted and the formazan product was solubilized with 200 μL of DMSO. Blank wells contained only medium and MTT. Absorbance was measured at 590 nm with a reference wavelength of 690 nm.

DNA Synthesis Assay

The Click-iT EdU DNA assay was performed according to the manufacturer's recommended protocol. First, cells were exposed to EdU at a concentration of 10 µM for 2 h. Cells were then fixed, permeabilized, and labelled with Alexa Fluor 642 via a click chemistry reaction. Cells were immediately analyzed by flow cytometry.

Statistical Analyses

Statistical analyses were performed using Microsoft Excel 2010 suite. Flow cytometry data were analyzed using Origin Pro.

RESULTS AND DISCUSSION

Preparation and Characterization of PEGylated Au NPs

There are many different surface functionalization schemes that may be used to produce stable Au NPs. Some of the most commonly used molecules for this purpose are polymers (e.g., polyvinylpyrrolidone or polyethylene glycol) because of their ability to sterically protect

against aggregation (Zhang, 2009; Zhu, 2017). Other important functionalizing molecules include DNA aptamers (Yang, 2011), peptides (Field, 2015; Tkachenko, 2003), proteins (Brewer, 2005), and small molecules such as glutathione (Lu, 2012; Ghosh, 2008), all of which may provide steric or electrostatic stabilization. For this work, we chose to use polyethylene glycol as a coating agent due to the ease of preparation, biocompatibility, and clinical relevance of this type of nanoparticle conjugate. Because of the robust nature of the gold-sulfur bond (>200 kJ mol⁻¹) it can be prepared easily by mixing solutions of thiolated PEG and citrate-capped Au NPs at room temperature. Subsequent centrifugation and washing with distilled water yields stable, functionalized nanoparticles. There are many papers that use similar Au NP cores and PEG coatings for radiosensitization applications—albeit in epithelial cell lines— and published data usually show the trend of modest radiosensitization (SER ≥ 1.2) (Butterworth, 2012). In addition to its ability to stabilize Au NPs in vitro, polyethylene glycol is a powerful anti-biofouling agent. Au NPs coated in PEG are stable in serum, exhibit longer biological half-lives, and show less uptake by immune cells such as macrophages (Amoozgar and Yeo 2012).

We prepared PEGylated Au NPs through standard thiol-gold chemistry. Different ratios of amine- and methoxy-functionalized PEG were screened (Fig. S1) to determine an ideal ratio for radiosensitization studies. Based on these data, we used an 87:13 ratio of methoxy to amine terminated PEG because this combination has the desired balance of colloidal stability as well as the presence of reactive amine groups for fluorophore conjugation. These data agree with the known propensity of citrate-capped Au NPs to aggregate in the presence of cationic ligands, due to charge neutralization and subsequent loss of electrostatic repulsion. The Au NPs show minimal change in the surface plasmon resonance peak position during functionalization, indicating good colloidal stability (Fig. 1a). The Au NPs increase in average hydrodynamic diameter from 11 \pm 1 nm to 22 \pm 2 nm after PEGylation as measured by dynamic light scattering (DLS) measurements, in line with the presence of a surface coating of PEG (representative histograms are shown in Fig 1b). The dramatic shift in hydrodynamic radius

indicates that the PEG molecules are oriented perpendicular to the surface, as is expected at a high surface coverage of polymer (Kolasinski, 2012). To monitor the uptake of the PEGylated NPs by confocal microscopy and flow cytometry, Cy5 was conjugated to the amine terminated polymers and verified by UV-Vis spectrophotometry (Fig. 1a). The UV-Vis spectrum shows the appearance of new absorbance peaks corresponding to those of free Cy5. Additionally, the PEGylated Au NPs were stable in both cell culture medium (RPMI 1640 supplemented with 10% fetal bovine serum) and 5 mM glutathione (Fig. S2) by UV-Vis analysis, indicating that serum proteins and reactive thiols in the intracellular medium do not appreciably displace PEG from the NPs and induce aggregation.

Uptake of PEGylated Au NPs

We quantified the uptake of PEGylated Au NPs into Jurkat D1.1 and HL-60 II cells using confocal microscopy, flow cytometry, and spectroscopic techniques. The distribution of Cy5-labelled NPs in Jurkat D1.1 and HL-60 II cells by confocal microscopy after a 24 h incubation period is shown in Fig. 2a-b. The Au NPs, in some instances, are colocalized in the nuclei of the Jurkat D1.1 cell line, while showing a perinuclear distribution in the HL-60 II cell line. Despite these microscopy results, we were not able to confirm nuclear uptake by any other technique, including ICP-AES of isolated nuclei (data not shown). These results likely indicate that the NPs had not crossed the nuclear pore complex and were instead located in close to the nucleus, but within the confocal section used for imaging (~0.5 μm). The NPs have a more uniform distribution in the HL-60 II cell line, compared to the Jurkat D1.1 cell line where the NPs only appear as discrete puncta.

The cellular uptake of Cy5 labelled NPs was confirmed by flow cytometry, representative histograms of which are shown in Fig. 2c-d. There is a substantial shift in far-red fluorescence intensity of cells treated with Cy5-labeled Au NPs compared to untreated controls (see Electronic Supplementary Information for flow cytometry gating schemes). Because the cells were washed prior to flow cytometric analysis, this shift in far-red fluorescence intensity

indicates the successful endocytosis of Cy5-labeled Au NPs into both cell lines. Furthermore, gold content analysis by ICP-AES showed that $3.0 \pm 1.0 \times 10^3$ and $6.9 \pm 0.6 \times 10^3$ NPs were internalized into HL-60 II and Jurkat D1.1 cells, respectively, after 24 h incubation (n = 3; mean ± standard error). We assayed the toxicity of PEGylated Au NPs by MTT and resazurin reduction assays (Fig. S3 and S4). The NPs were well-tolerated by the two cell lines over the low nanomolar range, indicating good biocompatibility. Although PEGylation leads to decreased uptake relative to, for example, citrate- or peptide-conjugated nanoparticles, it is not eliminated completely(Gu, 2009; Yuan, 2008; C.-J. Liu, 2008; Yook, 2016; Kim, 2011). Brandenberger et al. showed that this process occurred by active, energy-dependent processes such as clathrinand caveolae-mediated endocytosis; however, in many published cases the mechanism is not explicitly stated (Brandenberger, 2010). At least two published works have investigated the uptake and toxicity of nanomaterials in Jurkat cells—it was found that citrate capped Au NPs are well-tolerated over the micromolar range but that CTAB coating causes toxicity, starting at ~50 nM (Connor, 2005). However, CTAB is positively charged and is known to interact destructively with cell and organelle membranes, leading to profound toxicity (Kodiha, 2015). In contrast, zinc oxide nanoparticles are not toxic in the Jurkat cell line until concentrations above 0.1 mM.

Radiosensitization of Jurkat D1.1 and HL 60 II Cells

To date, there have been no published works showing radiosensitization of a leukemia cell line by colloidal nanoparticles. Despite this fact, the interactions of leukemia cells and nanomaterials have been investigated for other purposes, such as diagnosis and drug delivery (Soni, 2015). For example, poly(D,L-lactic-co-glycolic) acid nanoparticles have been used as carriers for anti-leukemia drugs such as cytarabine, doxorubicin, and 6-mercaptopurine to human leukemia cells in vitro (Danesh, 2015; Podsiadlo, 2008). Although not tested in vivo, these types of particles hold promise for increasing the biological half-life of chemotherapy drugs due to sustained release from the NP matrix. Because of the burgeoning interest in multimodal therapy (e.g., combination chemotherapy and radiation therapy), understanding the

effects of nanomaterials on radiosensitization are of utmost importance for future clinical utility of these particles (Setua, 2014; Cheon, 2008).

To determine whether there was a radiosensitizing effect of PEGylated Au NPs on either of these cell lines, we used electronic cell counting to measure survival of the cells following radiation exposure. Although the clonogenic survival assay is the most common test for proliferative ability, cell count is considered indicative of overall survival after five cell doubling times have accumulated, and is better suited for cells that grow in suspension (Freshney, 2010). To account for this modification, we plated cells at a low enough concentration that the control cells (non-irradiated) would be in the exponential phase of growth five days after irradiation. The dose response plots for Jurkat D1.1 and HL-60 II cells is shown in Fig. 3a and b; the data are the average of three biological replicates (i.e., separate NP batches, cell stocks, and irradiations), which were the average of three technical replicates each. The Jurkat D1.1 cell line (Fig. 3a) was radiation sensitive and appreciable cell death was observed at doses as low as 1 Gy. Despite this sensitivity, there were no statistically significant differences in survival between control populations and those exposed to Au NPs. The HL-60 II cell line (Fig. 3b) showed marked radiation resistance with a broad shoulder in the dose-response plots. Because p53 null cells, of which HL-60 II is included, are known to be especially resistant to apoptosis, these results can be explained by the unique cytogenetics of this cell line. However, with increasing dose, the populations of HL-60 II cells incubated with Au NPs showed statistically significant differences in growth compared to controls (4.3 \pm 0.1 vs 3.1 \pm 0.1 population doublings; p < 0.01 by Mann-Whitney U-test). One of the commonly used statistics to quantify the increased sensitivity of cells to ionizing radiation in the presence of Au NPs is the sensitivity enhancement ratio (SER), which represents the ratio of survival fractions at a particular radiation dose (Sancey, 2014). The other commonly used statistic is the dose enhancement factor (DEF), which represents the ratio of the area under the survival curves for control and NP treated

populations (Chithrani, 2010). We calculated the SER value for these cells lines by the following formula:

SER =
$$\frac{4 \text{ Gy Control}}{\frac{4 \text{ Gy NP Treated}}{0 \text{ Gy Control}}}$$
 (1)

which takes the ratio of cell counts for irradiated and non-irradiated populations. A SER value greater than 1 indicates radiosensitization, while a SER value less than 1 indicates radioprotection. This equation has the advantage of accounting for any inherent toxicity of the NPs, although we found that to be minimal in this case. According to this definition, the SER values at 5 Gy are 1.33 and 1.18 for the HL-60 II and Jurkat D1.1 cell lines, respectively. SER values for all radiation doses are summarized in Table 1.

As further corroboration of the radiosensitizing effects of PEGylated Au NPs, we measured the metabolic activity of the cells using an resazurin reduction assay (Fig. 4). This assay measures the ability of the cells to reduce resazurin into the fluorescent product resorufin, which correlates well with cell number and viability. The production of resorufin can be monitored by a plate reader and gives results that correlate well with those found by MTT and WST-8 assays (Marshall, 1995). Importantly, the resazurin reduction assay requires fewer centrifugation steps where cells may be lost and damaged and avoids some of the common pitfalls associated with solubilizing the formazan products of the traditional MTT assay. After a 5 Gy radiation dose, there is no statistically significant difference in resorufin production by control populations of Jurkat D1.1 cells and those exposed to Au NPs, in agreement with cell count data. For the HL-60 II cell line, in contrast, the data show a pronounced decrease in resorufin production for cells exposed to PEGylated Au NPs at 5 Gy (p < 0.001), indicating that very few cells have maintained a reducing environment within the cytosol and therefore that most cells are not viable. Because resazurin reduction has also shown good correlation with the clonogenic survival assay, these results further support the radiosensitizing effects of PEGylated Au NPs.

To better understand the radiosensitization effects of Au NPs, we assayed the cells by a DNA synthesis assay as shown in Fig. 5. By pulse labelling the cells with 5-ethynyl-2'-deoxyuridine (EdU), we were able to determine the percentage of cells that were actively synthesizing DNA (i.e., S phase cells) after a five-day growth period post irradiation. This assay is commonly used as a method for determining cell survival, especially when the clonogenic survival assay cannot be used (Simon, 2016; Derda, 2009). While we label this population as "S phase," an equally appropriate label is "proliferating cells" because this population has entered the cell cycle is actively making new DNA (see Fig. S6 for representative gating schemes).

The percentage of S phase cells after a two-hour labelling period with EdU is shown in Fig. 5 for both cell lines. After a dose of 5 Gy, Jurkat D1.1 control cells and those incubated with Au NPs have S phase populations of $1.8\pm0.5\%$ and $2.4\pm0.1\%$, respectively, with no statistical significance between these populations of cells (p = 0.11). For HL-60 II cells, populations of cells incubated with NPs and irradiated have S phase populations of $3.9\pm0.1\%$ versus $0.16\pm0.03\%$ for cells that were not exposed to Au NPs (p < 0.001). While the number of cells in culture is on average 2.3 times less in the populations of cells exposed to Au NPs, the DNA synthesis assay indicates that the damage to the cells is much more severe than what is captured by cell count alone. Moreover, although the difference between 3.9% and 0.16% S phase populations may be small in absolute magnitude, it has profound implications for radiation therapy, where multiple logarithms of cell killing is necessary to ensure complete eradication of a tumor (Pawlik, 2004). The combination of these three tests (cell count, resazurin reduction, and DNA synthesis) unambiguously shows a common trend of decreased reproductive potential for HL-60 II cells irradiated in the presence of PEGylated Au NPs.

The differences in SER values for these two cell lines cannot be explained by a physical mechanism alone because there are, on average, more nanoparticles in the Jurkat D1.1 cell line than the HL-60 II cell line at the time of irradiation. While the original theories explaining Au NP radiosensitization were based solely on X-ray absorption and the local production of

photoelectrons, there is now substantial evidence that biological processes can affect the radiation response (Rosa, 2017). For example, Au NPs have been shown to have an epigenetic effect on mammalian cells, increasing the concentration of proteins (e.g., thymidylate synthetase), that are implicated in cell survival following insult (Turnbull, 2019; Falagan-Lotsch, 2016). Another potential biological mechanism is through the induction of autophagy, a type of programmed cell death that involves the lysosomal destruction of organelles, sometimes referred to as "self-eating," (White, 2015; Onorati, 2018) and which is known to alter survival following radiation exposure (Paglin, 2001; Apel, 2008). Au NPs and other metal nanoparticles have been shown to induce autophagy in many cell lines in vitro, and biological processes such as this may be a factor in the differential SER values observed in this work (Ma, 2011; Li, 2010). Another biological consideration is the cytogenetics of the cell line under investigation, especially any mutations or deletions in genes known to be involved in the radiation response. The HL-60 II cell line, unlike Jurkat D1.1, is p53 null and the dominant mechanism of cell death is mitotic catastrophe (Vakifahmetoglu, 2008; Castedo, 2004; Vitale, 2011). This mode of cell death usually takes many cell divisions to result in a failed mitosis, which could account for the relatively high cell numbers for the HL-60 II cell line, and the corresponding decrease in metabolic activity and DNA synthesis. Other mechanisms of Au NP radiosensitization are related to surface reactions catalyzed by the metal core of the nanoparticle, such as the production of reactive oxygen species (ROS) (Pan, 2009). Interestingly, a recent paper found that purely amino-terminated Au NPs induced mitochondrial stress in HL-60 cells, leading to cytoxicity and other downstream biological consequences (Gaiser, 2019).

Due to the variability in nanoparticle formulation, working concentration, cell lines, and irradiation energies, it is difficult to directly compare the results of Au NP radiosensitization studies between different research groups. Recent commentary on the translation of heavy metal nanoparticles to clinical settings has identified this as a major hurdle in identifying common trends in heavy metal nanoparticle therapeutics. Nevertheless, at least two published

works have used Au NPs coated in PEG to radiosensitize epithelial cells to ionizing radiation. Liu et al. showed a maximum SER of 2 for CT-26 cells at a concentration of 1 mM with a 6 keV electron source (C.-J. Liu et al., 2010). As the authors note, this enhancement effect cannot be attributed solely to the increase in local energy deposition by Au NPs, which hints at an additional biological mechanism of radiation damage, in agreement with the results of this paper. This conclusion has also been reached in other studies of Au NP radiosensitization and is an active area of research in the field. In another paper by this same group, the radiosensitizing effect of PEGylated Au NPs was confirmed in CT-26 cells by synchrotron FTIR measurements, which showed substantial spectral changes in C=O bond stretches in cells irradiated in the presence of NPs, which they interpreted as indicative of apoptosis (C.-J. Liu et al., 2008). One earlier work investigated the effect of layering primary T-cells on a gold foil on the relative biological effectiveness of X-ray irradiation. The authors found a substantial increase in chromosomal aberrations in the presence of a gold foil, despite a distance between foil and nucleus of several micrometers (Regulla et al., 2002). The ability of PEGylated Au NPs to radiosensitize an acute promyelocytic leukemia cell line-with known radiation resistance-at such a low concentration and internalized number of NPs (<104 per cell) bodes well for the ability of this NP formulation to be used in vivo as a radiosensitizer, where high concentrations of Au NPs may be difficult to achieve, or may have unforeseen toxicities.

CONCLUSION

In summary, we have demonstrated that polyethylene glycol-coated Au NPs can radiosensitize a leukemia cell line at nanomolar concentrations. The PEGylated NPs are easy to prepare, monodisperse, and stable against aggregation, even with extended incubations in cell culture medium. In this work, we have shown that the PEGylated NPs are taken up to a similar extent in both cell lines; however, in the HL-60 II cell line, their presence leads to dramatically different radiosensitization behavior. Importantly, PEGylated Au NPs are one of the best

candidates for eventual transition to clinical settings, due to the favorable anti-biofouling and stealth properties of this surface coating (Rabe, Verdes, and Seeger, 2011). Although the NPs are non-targeted, particles of this type are taken up by tumors due to the EPR effect. Particles of this type may also be injected into the tumor volume itself, allowing for a higher local concentration of particles (Yook et al., 2016). Moreover, the ease of production of PEGylated Au NPs allows for easy scale-up.

ACKNOWLEDGEMENTS

The authors gratefully acknowledge Mike Zurawski and Tara Medich (Massachusetts General Hospital) for assistance with irradiation experiments, Prof. Samuel Thomas for access to dynamic light scattering instrument, and Prof. Sangeeta Bhatia and Dr. Alex Albanese (Massachusetts Institute of Technology) for helpful conversations and advice on nanoparticle design. We thank Dr. Michael Pawlita (DFKZ German Cancer Research Center) for providing the HL-60 II cell line. This work was supported by The National Science Foundation (CHE-1708397) and a Research Corporation for Science SEED Award granted to Prof. Charles Sykes.

ETHICS DECLARATION

Conflict of interest

The authors declare that they have no conflict of interest.

REFERENCES

Alizadeh, E., T. M. Orlando, and Léon Sanche. 2015. "Biomolecular Damage Induced by Ionizing Radiation: The Direct and Indirect Effects of Low-Energy Electrons on DNA."

Annual Review of Physical Chemistry 66 (1): 379–98. https://doi.org/10.1146/annurev-physchem-040513-103605.

- Amoozgar, Zohreh, and Yoon Yeo. 2012. "Recent Advances in Stealth Coating of Nanoparticle

 Drug Delivery Systems." Wiley Interdisciplinary Reviews: Nanomedicine and

 Nanobiotechnology 4 (2): 219–33. https://doi.org/10.1002/wnan.1157.
- Apel, Anja, Ingrid Herr, Heinz Schwarz, H. Peter Rodemann, and Andreas Mayer. 2008.

 "Blocked Autophagy Sensitizes Resistant Carcinoma Cells to Radiation Therapy." *Cancer Research* 68 (5): 1485–94. https://doi.org/10.1158/0008-5472.CAN-07-0562.
- Berbeco, Ross I., Houari Korideck, Wilfred Ngwa, Rajiv Kumar, Janki Patel, Srinivas Sridhar, Sarah Johnson, Brendan D. Price, Alec Kimmelman, and G. Mike Makrigiorgos. 2012.
 "DNA Damage Enhancement from Gold Nanoparticles for Clinical MV Photon Beams."

 Radiation Research 178 (6): 604–8. https://doi.org/10.1667/RR3001.1.
- Brandenberger, Christina, Christian Mühlfeld, Zulqumain Ali, Anke Gabriele Lenz, Otmar Schmid, Wolfgang J. Parak, Peter Gehr, and Barbara Rothen-Rutishauser. 2010.

 "Quantitative Evaluation of Cellular Uptake and Trafficking of Plain and Polyethylene Glycol-Coated Gold Nanoparticles." *Small* 6 (15): 1669–78.

 https://doi.org/10.1002/smll.201000528.
- Brewer, Scott H., Wilhelm R. Glomm, Marcus C. Johnson, Magne K. Knag, and Stefan Franzen.

 2005. "Probing BSA Binding to Citrate-Coated Gold Nanoparticles and Surfaces." *Langmuir*21 (20): 9303–7. https://doi.org/10.1021/la050588t.
- Butterworth, Karl T, Stephen J McMahon, Fred J Currell, and Kevin M Prise. 2012. "Physical Basis and Biological Mechanisms of Gold Nanoparticle Radiosensitization." *Nanoscale* 4 (16): 4830–38. https://doi.org/10.1039/c2nr31227a.
- Castedo, Maria, Jean Luc Perfettini, Thomas Roumier, Karine Andreau, Rene Medema, and Guido Kroemer. 2004. "Cell Death by Mitotic Catastrophe: A Molecular Definition."

 Oncogene 23 (16 REV. ISS. 2): 2825–37. https://doi.org/10.1038/sj.onc.1207528.

- Cheon, Jinwoo, and Jae Hyun Lee. 2008. "Synergistically Integrated Nanoparticles as Multimodal Probes for Nanobiotechnology." *Accounts of Chemical Research* 41 (12): 1630–40. https://doi.org/10.1021/ar800045c.
- Chithrani, B Devika, Salomeh Jelveh, Farid Jalali, Monique van Prooijen, Christine Allen, Robert G Bristow, Richard P Hill, and David a Jaffray. 2010. "Gold Nanoparticles as Radiation Sensitizers in Cancer Therapy." *Radiation Research* 173 (6): 719–28. https://doi.org/10.1667/RR1984.1.
- Connor, Ellen E., Judith Mwamuka, Anand Gole, Catherine J. Murphy, and Michael D. Wyatt. 2005. "Gold Nanoparticles Are Taken up by Human Cells but Do Not Cause Acute Cytotoxicity." *Small* 1 (3): 325–27. https://doi.org/10.1002/smll.200400093.
- Danesh, Noor Mohammad, Parirokh Lavaee, Mohammad Ramezani, Khalil Abnous, and Seyed Mohammad Taghdisi. 2015. "Targeted and Controlled Release Delivery of Daunorubicin to T-Cell Acute Lymphoblastic Leukemia by Aptamer-Modified Gold Nanoparticles."

 International Journal of Pharmaceutics 489 (1–2): 311–17.

 https://doi.org/10.1016/j.ijpharm.2015.04.072.
- Derda, R., A. Laromaine, a. Mammoto, S. K. Y. Tang, T. Mammoto, D. E. Ingber, and G. M. Whitesides. 2009. "Paper-Supported 3D Cell Culture for Tissue-Based Bioassays."

 Proceedings of the National Academy of Sciences 106 (44): 18457–62.

 https://doi.org/10.1073/pnas.0910666106.
- Duvic, Madeleine, Michele Donato, Bouthaina Dabaja, Heather Richmond, Lotika Singh, Wei Wei, Sandra Acholonu, Issa Khouri, Richard Champlin, and Chitra Hosing. 2010. "Total Skin Electron Beam and Non-Myeloablative Allogeneic Hematopoietic Stem-Cell Transplantation in Advanced Mycosis Fungoides and S??Zary Syndrome." *Journal of Clinical Oncology* 28 (14): 2365–72. https://doi.org/10.1200/JCO.2009.25.8301.

- Falagan-Lotsch, Priscila, Elissa M. Grzincic, and Catherine J. Murphy. 2016. "One Low-Dose Exposure of Gold Nanoparticles Induces Long-Term Changes in Human Cells."

 Proceedings of the National Academy of Sciences of the United States of America 113

 (47): 13318–23. https://doi.org/10.1073/pnas.1616400113.
- Field, Lauren D., James B. Delehanty, Yungchia Chen, and Igor L. Medintz. 2015. "Peptides for Specifically Targeting Nanoparticles to Cellular Organelles: Quo Vadis?" *Accounts of Chemical Research* 48 (5): 1380–90. https://doi.org/10.1021/ar500449v.
- Freshney, R. Ian. 2010. *Culture of Animal Cells*. 6th ed. Hoboken: John Wiley & Sons, Inc. https://doi.org/10.1002/9780471747598.
- Gaiser, Ann-Kathrin, Susanne Hafner, Michael Schmiech, Berthold Büchele, Patrick Schäfer, Christine A. Arnim, Enrico Calzia, et al. 2019. "Gold Nanoparticles with Selective Antileukemic Activity In Vitro and In Vivo Target Mitochondrial Respiration." *Advanced Therapeutics* 2 (6): 1800149. https://doi.org/10.1002/adtp.201800149.
- Ghosh, Partha, Gang Han, Mrinmoy De, Chae Kyu Kim, and Vincent M. Rotello. 2008. "Gold Nanoparticles in Delivery Applications." *Advanced Drug Delivery Reviews* 60: 1307–15. https://doi.org/10.1016/j.addr.2008.03.016.
- Gu, Yan Juan, Jinping Cheng, Chun Chi Lin, Yun Wah Lam, Shuk Han Cheng, and Wing Tak Wong. 2009. "Nuclear Penetration of Surface Functionalized Gold Nanoparticles." *Toxicology and Applied Pharmacology* 237 (2): 196–204. https://doi.org/10.1016/j.taap.2009.03.009.
- Guo, Jianfeng, Mary R. Cahill, Sharon L. McKenna, and Caitriona M. O'Driscoll. 2014.
 "Biomimetic Nanoparticles for SiRNA Delivery in the Treatment of Leukaemia."
 Biotechnology Advances 32 (8): 1396–1409.
 https://doi.org/10.1016/j.biotechadv.2014.08.007.

- Gupta, V., M. S. Tallman, and D. J. Weisdorf. 2011. "Allogeneic Hematopoietic Cell Transplantation for Adults with Acute Myeloid Leukemia: Myths, Controversies, and Unknowns." *Blood Journal* 117 (8): 2307–18. https://doi.org/10.1182/blood-2010-10-265603.
- Hainfeld, James F, F Avraham Dilmanian, Daniel N Slatkin, and Henry M Smilowitz. 2008. "Radiotherapy Enhancement with Gold Nanoparticles." *The Journal of Pharmacy and Pharmacology* 60 (8): 977–85. https://doi.org/10.1211/jpp.60.8.0005.
- Her, Sohyoung, David A. Jaffray, and Christine Allen. 2017. "Gold Nanoparticles for Applications in Cancer Radiotherapy: Mechanisms and Recent Advancements." Advanced Drug Delivery Reviews 109: 84–101. https://doi.org/10.1016/j.addr.2015.12.012.
- Hughes, Charlotte F M, Amit Khot, Christopher McCormack, Stephen Lade, David a.
 Westerman, Robert Twigger, Odette Buelens, et al. 2015. "Lack of Durable Disease
 Control with Chemotherapy for Mycosis Fungoides and S??Zary Syndrome: A
 Comparative Study of Systemic Therapy." *Blood* 125 (1): 71–81.
 https://doi.org/10.1182/blood-2014-07-588236.
- Jain, S., D. G. Hirst, and J. M. O'Sullivan. 2012. "Gold Nanoparticles as Novel Agents for Cancer Therapy." *British Journal of Radiology* 85 (1010): 101–13. https://doi.org/10.1259/bjr/59448833.
- Keppler, O. T. 1999. "UDP-GlcNAc 2-Epimerase: A Regulator of Cell Surface Sialylation." Science 284 (5418): 1372–76. https://doi.org/10.1126/science.284.5418.1372.
- Kim, Young Hwa, Jongho Jeon, Su Hyun Hong, Won Kyu Rhim, Yun Sang Lee, Hyewon Youn, June Key Chung, et al. 2011. "Tumor Targeting and Imaging Using Cyclic RGD-PEGylated Gold Nanoparticle Probes with Directly Conjugated Iodine-125." *Small* 7: 2052–60. https://doi.org/10.1002/smll.201100927.

- Kodiha, Mohamed, Yi Meng Wang, Eliza Hutter, Dusica Maysinger, and Ursula Stochaj. 2015.

 "Off to the Organelles Killing Cancer Cells with Targeted Gold Nanoparticles."

 Theranostics 5 (4): 357–70. https://doi.org/10.7150/thno.10657.
- Kolasinski, Kurt. 2012. Surface Science: Foundations of Catalysis and Nanoscience. Wiley.
- Kouass Sahbani, S., P. Cloutier, A. D. Bass, D. J. Hunting, and L. Sanche. 2015. "Electron Resonance Decay into a Biological Function: Decrease in Viability of *E. Coli* Transformed by Plasmid DNA Irradiated with 0.5–18 EV Electrons." *The Journal of Physical Chemistry Letters* 6 (19): 3911–14. https://doi.org/10.1021/acs.jpclett.5b01585.
- Li, Jasmine J., Deny Hartono, Choon Nam Ong, Boon Huat Bay, and Lin Yue L. Yung. 2010. "Autophagy and Oxidative Stress Associated with Gold Nanoparticles." *Biomaterials* 31 (23): 5996–6003. https://doi.org/10.1016/j.biomaterials.2010.04.014.
- Liu, Chi-Jen, Chang-Hai Wang, Shin-Tai Chen, Hsiang-Hsin Chen, Wei-Hua Leng, Chia-Chi Chien, Cheng-Liang Wang, et al. 2010. "Enhancement of Cell Radiation Sensitivity by Pegylated Gold Nanoparticles." *Physics in Medicine and Biology* 55 (4): 931–45. https://doi.org/10.1088/0031-9155/55/4/002.
- Liu, Chi-Jen, Chang-Hai Wang, Chia-Chi Chien, Tsung-Yeh Yang, Shin-Tai Chen, Wei-Hua Leng, Cheng-Feng Lee, et al. 2008. "Enhanced X-Ray Irradiation-Induced Cancer Cell Damage by Gold Nanoparticles Treated by a New Synthesis Method of Polyethylene Glycol Modification." *Nanotechnology* 19 (29): 295104. https://doi.org/10.1088/0957-4484/19/29/295104.
- Liu, Jiawen, Xiaobin Yao, Pierre Cloutier, Yi Zheng, and Léon Sanche. 2015. "DNA Strand Breaks Induced by 0–1.5 EV UV Photoelectrons under Atmospheric Pressure." *The Journal of Physical Chemistry C*, acs.jpcc.5b11072. https://doi.org/10.1021/acs.jpcc.5b11072.

- Lu, Yan, Lixia Wang, Dejun Chen, and Gongke Wang. 2012. "Determination of the Concentration and the Average Number of Gold Atoms in a Gold Nanoparticle by Osmotic Pressure." *Langmuir* 28 (25): 9282–87. https://doi.org/10.1021/la300893e.
- Ma, Xiaowei, Yanyang Wu, Shubin Jin, Yuan Tian, Xiaoning Zhang, Yuliang Zhao, Li Yu, and Xing Jie Liang. 2011. "Gold Nanoparticles Induce Autophagosome Accumulation through Size-Dependent Nanoparticle Uptake and Lysosome Impairment." *ACS Nano* 5 (11): 8629–39. https://doi.org/10.1021/nn202155y.
- Marshall, N.J., C.J. Goodwin, and S.J. Holt. 1995. "Marshall et Al-Growth and Regulation-1995.Pdf." *Growth and Regulation* 5 (2): 69–84.
- Ngwa, Wilfred, Houari Korideck, Amin I. Kassis, Rajiv Kumar, Srinivas Sridhar, G. Mike Makrigiorgos, and Robert a. Cormack. 2013. "In Vitro Radiosensitization by Gold Nanoparticles during Continuous Low-Dose-Rate Gamma Irradiation with I-125 Brachytherapy Seeds." *Nanomedicine: Nanotechnology, Biology, and Medicine* 9 (1): 25–27. https://doi.org/10.1016/j.nano.2012.09.001.
- Onorati, Angelique V., Matheus Dyczynski, Rani Ojha, and Ravi K. Amaravadi. 2018. "Targeting Autophagy in Cancer." *Cancer* 124 (16): 3307–18. https://doi.org/10.1002/cncr.31335.
- Paglin, Shoshana, Timothy Hollister, Thomas Delohery, Nadia Hackett, Melissa McMahill, Eleana Sphicas, Diane Domingo, and Joachim Yahalom. 2001. "A Novel Response of Cancer Cells to Radiation Involves Autophagy and Formation of Acidic Vesicles." *Cancer Research* 61 (2): 439–44.
- Pan, Yu, Annika Leifert, David Ruau, Sabine Neuss, Jörg Bornemann, Günter Schmid, Wolfgang Brandau, Ulrich Simon, and Willi Jahnen-Dechent. 2009. "Gold Nanoparticles of Diameter 1.4 Nm Trigger Necrosis by Oxidative Stress and Mitochondrial Damage." *Small* 5 (18): 2067–76. https://doi.org/10.1002/smll.200900466.

- Pan, Yu, Sabine Neuss, Annika Leifert, Monika Fischler, Fei Wen, Ulrich Simon, Günter Schmid, Wolfgang Brandau, and Willi Jahnen-Dechent. 2007. "Size-Dependent Cytotoxicity of Gold Nanoparticles." *Small* 3 (11): 1941–49. https://doi.org/10.1002/smll.200700378.
- Pawlik, Timothy M., and Khandan Keyomarsi. 2004. "Role of Cell Cycle in Mediating Sensitivity to Radiotherapy." *International Journal of Radiation Oncology Biology Physics* 59 (4): 928–42. https://doi.org/10.1016/j.ijrobp.2004.03.005.
- Podsiadlo, Paul, Vladimir a. Sinani, Joong Hwan Bahng, Nadine Wong Shi Kam, Jungwoo Lee, and Nicholas a. Kotov. 2008. "Gold Nanoparticles Enhance the Anti-Leukemia Action of a 6-Mercaptopurine Chemotherapeutic Agent." *Langmuir* 24 (2): 568–74. https://doi.org/10.1021/la702782k.
- Rabe, Michael, Dorinel Verdes, and Stefan Seeger. 2011. "Understanding Protein Adsorption Phenomena at Solid Surfaces." *Advances in Colloid and Interface Science* 162 (1–2): 87–106. https://doi.org/10.1016/j.cis.2010.12.007.
- Regulla, D, E Schmid, W Friedland, W Panzer, U Heinzmann, and D Harder. 2002. "Enhanced Values of the RBE and H Ratio for Cytogenetic Effects Induced by Secondary Electrons from an X-Irradiated Gold Gurface." *Radiation Research* 158 (4): 505–15. https://doi.org/10.1667/0033-7587.
- Roa, Wilson, Xiaojing Zhang, Linghong Guo, Andrew Shaw, Xiuying Hu, Yeping Xiong, Sunil Gulavita, et al. 2009. "Gold Nanoparticle Sensitize Radiotherapy of Prostate Cancer Cells by Regulation of the Cell Cycle." *Nanotechnology* 20 (37): 375101. https://doi.org/10.1088/0957-4484/20/37/375101.
- Rosa, Soraia, Chris Connolly, Giuseppe Schettino, Karl T. Butterworth, and Kevin M. Prise.

 2017. "Biological Mechanisms of Gold Nanoparticle Radiosensitization." *Cancer Nanotechnology* 8 (1). https://doi.org/10.1186/s12645-017-0026-0.

- Sancey, L, F Lux, S Kotb, S Roux, S Dufort, a Bianchi, Y Crémillieux, et al. 2014. "The Use of Theranostic Gadolinium-Based Nanoprobes to Improve Radiotherapy Efficacy." *The British Journal of Radiology* 87 (1041): 20140134. https://doi.org/10.1259/bjr.20140134.
- Schuemann, Jan, Ross Berbeco, Devika B. Chithrani, Sang Hyun Cho, Rajiv Kumar, Stephen J. McMahon, Srinivas Sridhar, and Sunil Krishnan. 2016. "Roadmap to Clinical Use of Gold Nanoparticles for Radiation Sensitization." *International Journal of Radiation Oncology Biology Physics* 94 (1): 189–205. https://doi.org/10.1016/j.ijrobp.2015.09.032.
- Setua, Sonali, Myriam Ouberai, Sara G. Piccirillo, Colin Watts, and Mark Welland. 2014. "Cisplatin-Tethered Gold Nanospheres for Multimodal Chemo-Radiotherapy of Glioblastoma." *Nanoscale* 6: 10865–73. https://doi.org/10.1039/C4NR03693J.
- Simon, Karen a., Bobak Mosadegh, Kyaw Thu Minn, Matthew R. Lockett, Marym R.

 Mohammady, Diane M. Boucher, Amy B. Hall, et al. 2016. "Metabolic Response of Lung

 Cancer Cells to Radiation in a Paper-Based 3D Cell Culture System." *Biomaterials* 95: 47–
 59. https://doi.org/10.1016/j.biomaterials.2016.03.002.
- Soni, Govind, and Khushwant S. Yadav. 2015. "Applications of Nanoparticles in Treatment and Diagnosis of Leukemia." *Materials Science and Engineering C* 47: 156–64. https://doi.org/10.1016/j.msec.2014.10.043.
- Tkachenko, Alexander G., Huan Xie, Donna Coleman, Wilhelm Glomm, Joseph Ryan, Miles F.
 Anderson, Stefan Franzen, and Daniel L. Feldheim. 2003. "Multifunctional Gold
 Nanoparticle-Peptide Complexes for Nuclear Targeting." *Journal of the American Chemical Society* 125 (16): 4700–4701. https://doi.org/10.1021/ja0296935.
- Tsimberidou, a-M, H M Kantarjian, E Estey, J E Cortes, S Verstovsek, S Faderl, D a Thomas, et al. 2003. "Outcome in Patients with Nonleukemic Granulocytic Sarcoma Treated with Chemotherapy with or without Radiotherapy." *Leukemia* 17 (6): 1100–1103.

- https://doi.org/10.1038/sj.leu.2402958.
- Turnbull, Tyron, Michael Douglass, Nathan H. Williamson, Douglas Howard, Richa Bhardwaj, Mark Lawrence, David J. Paterson, Eva Bezak, Benjamin Thierry, and Ivan M. Kempson. 2019. "Cross-Correlative Single-Cell Analysis Reveals Biological Mechanisms of Nanoparticle Radiosensitization." Research-article. ACS Nano 13 (5): 5077–90. https://doi.org/10.1021/acsnano.8b07982.
- Uckun, Fatih M., Dorothea E. Myers, Jianjun Cheng, and Sanjive Qazi. 2015. "Liposomal Nanoparticles of a Spleen Tyrosine Kinase P-Site Inhibitor Amplify the Potency of Low Dose Total Body Irradiation Against Aggressive B-Precursor Leukemia and Yield Superior Survival Outcomes in Mice." *EBioMedicine* 2 (6): 554–62. https://doi.org/10.1016/j.ebiom.2015.04.005.
- Uckun, Fatih M., Dorothea E. Myers, Hong Ma, Rebecca Rose, and Sanjive Qazi. 2015. "Low Dose Total Body Irradiation Combined With Recombinant CD19-Ligand×Soluble TRAIL Fusion Protein Is Highly Effective Against Radiation-Resistant B-Precursor Acute Lymphoblastic Leukemia in Mice." *EBioMedicine* 2 (4): 306–16. https://doi.org/10.1016/j.ebiom.2015.02.008.
- Ulman, A. 1996. "Formation and Structure of Self-Assembled Monolayers." *Chemical Reviews* 96 (4): 1533–54. https://doi.org/10.1021/cr9502357.
- Vakifahmetoglu, H., M. Olsson, and B. Zhivotovsky. 2008. "Death through a Tragedy: Mitotic Catastrophe." *Cell Death and Differentiation* 15 (7): 1153–62. https://doi.org/10.1038/cdd.2008.47.
- Vericat, C, M E Vela, G Benitez, P Carro, and R C Salvarezza. 2010. "Self-Assembled Monolayers of Thiols and Dithiols on Gold: New Challenges for a Well-Known System."

 Chemical Society Reviews 39 (5): 1805–34. https://doi.org/10.1039/b907301a.

- Vitale, Ilio, Lorenzo Galluzzi, Maria Castedo, and Guido Kroemer. 2011. "Mitotic Catastrophe: A Mechanism for Avoiding Genomic Instability." *Nature Reviews. Molecular Cell Biology* 12 (6): 385–92. https://doi.org/10.1038/nrm3115.
- White, Eileen. 2015. "The Role for Autophagy in Cancer (White, 2015).Pdf." *Journal of Clinical Investigation* 125 (1): 42–46. https://doi.org/10.1172/JCI73941.Autophagy.
- Wiernik, P H, P L Banks, D C Case, Z a Arlin, P O Periman, M B Todd, P S Ritch, R E Enck, and a B Weitberg. 1992. "Cytarabine plus Idarubicin or Daunorubicin as Induction and Consolidation Therapy for Previously Untreated Adult Patients with Acute Myeloid Leukemia." *Blood* 79 (2): 313–19. https://doi.org/1730080.
- Yang, Liu, Xiaobing Zhang, Mao Ye, Jianhui Jiang, Ronghua Yang, Ting Fu, Yan Chen, Kemin Wang, Chen Liu, and Weihong Tan. 2011. "Aptamer-Conjugated Nanomaterials and Their Applications." *Advanced Drug Delivery Reviews* 63 (14–15): 1361–70. https://doi.org/10.1016/j.addr.2011.10.002.
- Yook, S., Z. Cai, Y. Lu, M. A. Winnik, J.-P. Pignol, and R. M. Reilly. 2016. "Intratumorally Injected 177Lu-Labeled Gold Nanoparticles Gold Nanoseed Brachytherapy with Application for Neo-Adjuvant Treatment of Locally Advanced Breast Cancer (LABC)."

 Journal of Nuclear Medicine 57 (6): 936–43. https://doi.org/10.2967/jnumed.115.168906.
- Yuan, Hong, Jing Miao, Yong Zhong Du, Jian You, Fu Qiang Hu, and Su Zeng. 2008. "Cellular Uptake of Solid Lipid Nanoparticles and Cytotoxicity of Encapsulated Paclitaxel in A549 Cancer Cells." *International Journal of Pharmaceutics* 348 (1–2): 137–45. https://doi.org/10.1016/j.ijpharm.2007.07.012.
- Zhang, Guodong, Zhi Yang, Wei Lu, Rui Zhang, Qian Huang, Mei Tian, Li Li, Dong Liang, and Chun Li. 2009. "Influence of Anchoring Ligands and Particle Size on the Colloidal Stability and in Vivo Biodistribution of Polyethylene Glycol-Coated Gold Nanoparticles in Tumor-

Xenografted Mice." *Biomaterials* 30 (10): 1928–36. https://doi.org/10.1016/j.biomaterials.2008.12.038.

Zhu, Lingying, Dawei Guo, Lili Sun, Zhihai Huang, Xiuyan Zhang, Wenjuan Ma, Jie Wu, Lun Xiao, Yun Zhao, and Ning Gu. 2017. "Activation of Autophagy by Elevated Reactive Oxygen Species Rather than Released Silver Ions Promotes Cytotoxicity of Polyvinylpyrrolidone-Coated Silver Nanoparticles in Hematopoietic Cells." *Nanoscale* 9 (17): 5489–98. https://doi.org/10.1039/C6NR08188F.

Fig. 1 Characterization of PEGylated Au NPs. (a) UV-Vis spectra at each stage of functionalization. The surface plasmon resonance remains unchanged during each step. (b) DLS histograms of the Au NPs with both citrate and PEG surfaces.

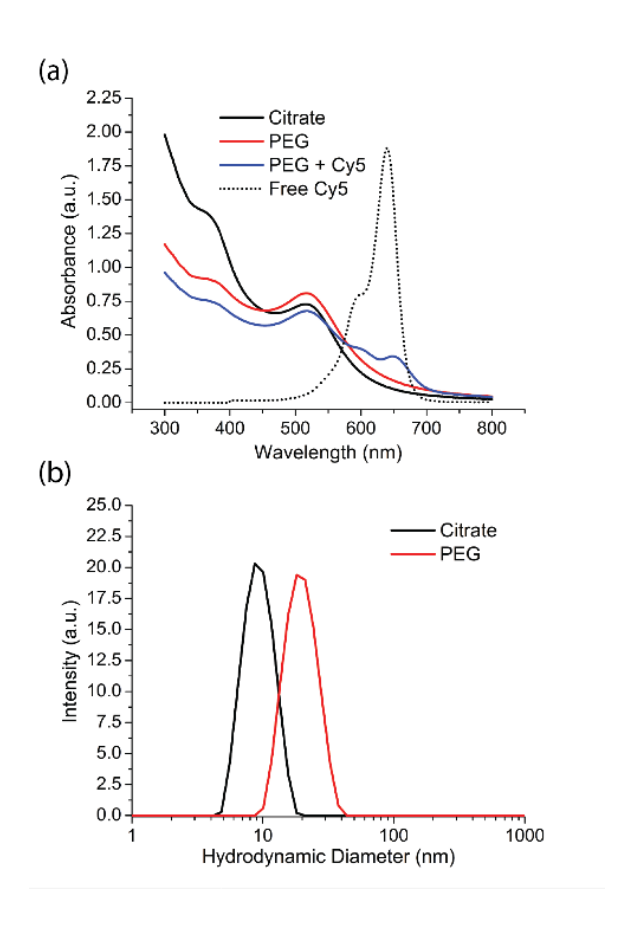


Fig. 2 Uptake of PEGylated Au NPs by Jurkat D1.1 and HL-60 II cells. Representative confocal microscopy images of (a) Jurkat D1.1 and (b) HL-60 II cells after 24 h incubation with PEGylated Au NPs (red = Cy5; blue = DAPI). Representative flow cytometry histograms of uptake of PEGylated Au NPs in (c) Jurkat D1.1 and (d) HL-60 II cells.

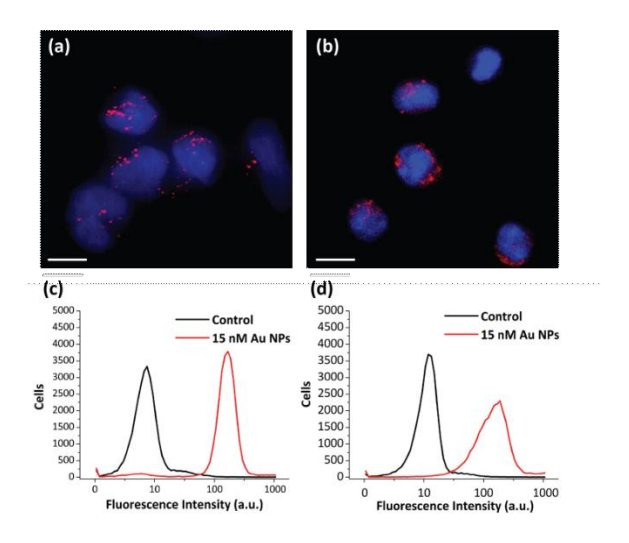


Fig. 3 Dose response data for (a) Jurkat D1.1 and (b) HL-60 II cells after a five-day growth period post-irradiation by electronic cell counting. The data are the average of three biological replicates. y-axis: log2 fold change in cell number, which represents the number of times the cells were able to double in population during the growth period, starting from 5,000 cells. Error bars represent standard error of the mean. (** p < 0.01 by Mann-Whitney U Test)

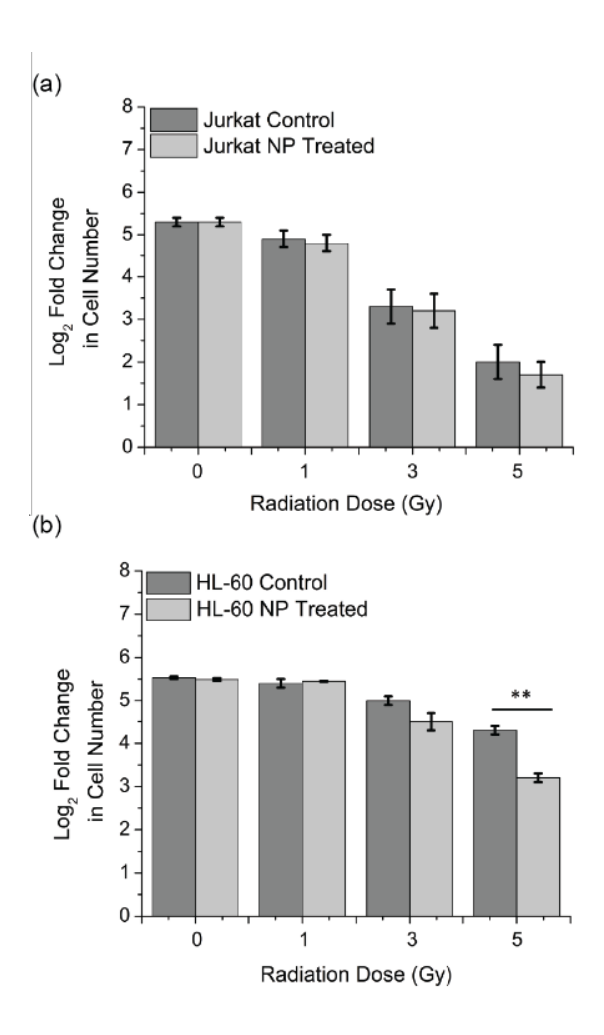


Fig. 4 Resazurin reduction assay for (a) Jurkat and (b) HL-60 cell lines from 0–5 Gy. The data are the average of three biological replicates \pm standard error of the mean. (* p < 0.05, *** p < 0.001 by Student's t-test). Fluorescence measurements were taken at 590 nm.

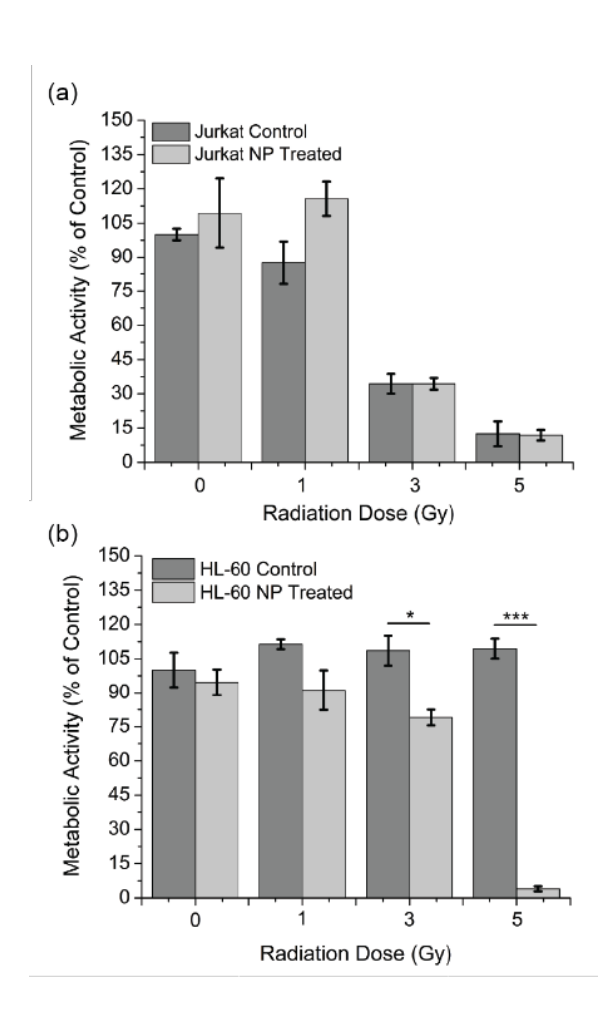


Table 1. Sensitivity enhancement ratios for HL-60 II and Jurkat cells at 15 nM nanoparticle concentration.

	SER		
	1 Gy	3 Gy	5 Gy
HL-60	0.98	1.10	1.33
Jurkat	1.02	1.03	1.18

Fig. 5 DNA synthesis assay. Percentages of S-phase cells were quantified by flow cytometry at 5 days post-irradiation. See Supplemental information for gating schemes and representative histograms (n = 3; error bars represent the standard deviation of mean; *** p < 0.001 by Student's t-test).

